J. Fluid Mech. (1975), *vol.* 68, *part* 1, *pp.* 109–128
Printed in Great Britain

An inviscid model of two-dimensional vortex shedding for transient and asymptotically steady separated flow over an inclined plate

By TURGUT SARPKAYA

Department of Mechanical Engineering, Naval Postgraduate School, Monterey, California 93940

(Received 18 October 1973 and in revised form 5 June 1974)

A potential flow model of two-dimensional vortex shedding behind an inclined plate is developed. The free shear layers which emanate from the sides of the plate are represented by discrete vortices through the use of the appropriate complex-velocity potential, the Kutta condition and the Joukowsky transformation between a circle and the plate cross-section. The analysis is then applied to predict the kinematic and dynamic characteristics of the flow for various angles of attack. The results compare favourably with the available experimental data as far as the form of vortex shedding and the Strouhal number are concerned. The calculated normal-force coefficients are 20–25% larger than those measured by Fage & Johansen (1927).

1. Introduction

In this paper an inviscid model of two-dimensional vortex shedding behind an inclined flat plate in the incidence range from approximately 30 to 90° is developed. The model uses an approximate representation of the continuous vortex sheets by an array of discrete vortices.

Following Rosenhead's (1931) pioneering work, numerous authors became interested in this method. Recently, Clements & Maull (1975) gave a nearly complete list of the previous applications of the discrete-vortex approximation and stated clearly both the utility and the limitations of the method. Here only those studies which have a direct bearing on the present work will be briefly described.

Kuwahara (1973), in a paper published after the initial submission of the present paper, studied two-dimensional vortex shedding behind an inclined flat plate through the use of the discrete-vortex approximation. The strengths of the point vortices were determined from the Kutta condition.† The vortices were introduced at two arbitrary fixed points near the edges of the plate. Kuwahara found that the calculated values of the normal-force coefficients were on the average 1·5–2 times larger than those obtained experimentally and that they exhibited sudden increases or decreases with amplitudes as large as four times the average value. He did not calculate the Strouhal numbers as no

† A referee has pointed out that Saks, Lundberg & Hansen (1967) have used a similar method to satisfy the Kutta condition.

periodic oscillations were discernible in his results. Through a parametric study of small variations in the point of appearance of the nascent vortices, Kuwahara also showed that not only the time of occurrence but also the amplitude of the oscillations of the normal-force coefficient strongly depend upon the assumed positions of the two fixed points. In fact, a small change in the position of the nascent vortices caused as much as an eightfold change in the normal-force coefficient. The present study shows that the difficulties encountered by Kuwahara are not a consequence of a deficiency of the method of discrete-vortex approximation but rather a consequence of the failure to recognize that the oscillation of the point of appearance of the vortices is of vital importance (Kronauer 1964) and is coupled with the manner in which the vortex sheets roll up. This fact, which has also been stressed by Gerrard (1967), has been ignored by all those who have satisfied the Kutta condition in similar studies of flows about bodies with salient edges (Clements & Maull 1975).

The discrete-vortex model of vortex shedding behind a square-based body described in Clements (1973) has been developed to include a Kutta condition similar to that used by this author, and to describe a number of further flow situations related to the original one (Clements & Maull 1975). The positions of the vortices chosen were in the planes of the body sides and a short distance downstream of the separation points. Clements & Maull (1975) discovered, by trial computations, that, if it was at a distance of between 0·005 and 0·015 times the base height, the exact point of appearance of the vortices did not affect the Strouhal number of the shedding, nor the form of vortex cluster formation. However, they were unable to predict a satisfactory unique base pressure since the vortex strength necessary to satisfy the Kutta condition and the rate of change of circulation necessary to calculate the base pressure depended upon the distance of the nascent vortex from the separation point. Evidently, the value of the model would be enhanced if the forces and pressures acting on the bodies under consideration could be accurately predicted. This in turn requires a satisfactory mechanism of feedback from wake fluctuations to the fluctuations in the rate of circulation (Kronauer 1964) and in turn in the position of appearance of the nascent vortices.

The work described herein introduces a number of improvements into the discrete-vortex representation of the shear layers, thereby eliminating the difficulties arising from the use of the Kutta condition and the occasional proximity of the point vortices. Both the rate at which vorticity is shed into the wake and the position at which this vorticity appears are allowed to vary with time.

2. Mathematical description of the model

Complex potential and the Kutta conditions

The calculation of the velocity of any one of the vortices and the normal force acting on the body requires a transformation plane (in which the plate becomes a circle), a complex-velocity potential representing the vortices and the two-dimensional irrotational flow around the body, and the use of the generalized Blasius theorem.

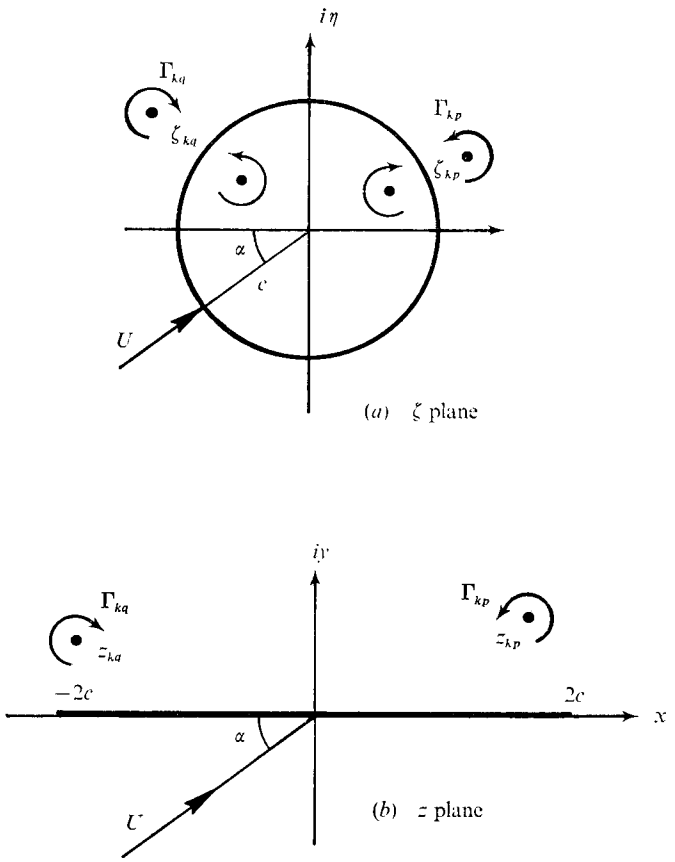

FIGURE 1. Flow in the (*a*) transformed and (*b*) physical planes.

The complex potential function w in the circle plane (see figure 1*a*) which describes a uniform flow U with a doublet at the origin to simulate the cylinder, $k+1$ vortices (rotating counterclockwise) on the right-hand side of the wake (called p-vortices), $k+1$ vortices (rotating clockwise) on the left-hand side of the wake (called q-vortices), and the images of all the p- and q-vortices in the circle may be written as

$$\begin{aligned} w(\zeta) = &-U\left(\zeta e^{-i\alpha}+\frac{c^2}{\zeta}e^{i\alpha}\right)+\frac{i\Gamma_{0p}}{2\pi}\log(\zeta-\zeta_{0p})-\frac{i\Gamma_{0p}}{2\pi}\log\left(\zeta-\frac{c^2}{\bar{\zeta}_{0p}}\right)\\ &+\sum_{k=1}^{m}\frac{i\Gamma_{kp}}{2\pi}\log(\zeta-\zeta_{kp})-\sum_{k=1}^{m}\frac{i\Gamma_{kp}}{2\pi}\log\left(\zeta-\frac{c^2}{\bar{\zeta}_{kp}}\right)-\frac{i\Gamma_{0q}}{2\pi}\log(\zeta-\zeta_{0q})\\ &+\frac{i\Gamma_{0q}}{2\pi}\log\left(\zeta-\frac{c^2}{\bar{\zeta}_{0q}}\right)-\sum_{k=1}^{m}\frac{i\Gamma_{kq}}{2\pi}\log(\zeta-\zeta_{kq})+\sum_{k=1}^{m}\frac{i\Gamma_{kq}}{2\pi}\log\left(\zeta-\frac{c^2}{\bar{\zeta}_{kq}}\right), \end{aligned} \tag{1}$$

in which Γ_{kp} and ζ_{kp} represent respectively the strength and location of the kth p-vortex, Γ_{kq} and ζ_{kq} the strength and location of the kth q-vortex, and c the radius of the cylinder; an overbar indicates a complex conjugate. The need for

the separate identification of the p- and q-vortices and for the singling out of one of the vortices in each shear layer (namely Γ_{0p} and Γ_{0q}) will become apparent later.

The flow in the circle plane may be transformed to that about an inclined plate by the Joukowsky transformation

$$z = \zeta + c^2/\zeta. \tag{2}$$

The fact that the flow separates tangentially at the edges of the plate (Kutta condition) may be expressed by requiring

$$dw/d\zeta = 0 \quad \text{at} \quad \zeta = \pm c, \tag{3}$$

which means that dw/dz gives a finite velocity at $z = \pm 2c$. Thus, inserting (1) in (3), one has

$$\begin{aligned} -U(e^{-i\alpha} - e^{i\alpha}) &+ \frac{i\Gamma_{0p}}{2\pi}\frac{1}{c-\zeta_{0p}} - \frac{i\Gamma_{0p}}{2\pi}\frac{1}{c-c^2/\bar{\zeta}_{0p}} + \sum_{k=1}^{m}\frac{i\Gamma_{kp}}{2\pi}\frac{1}{c-\zeta_{kp}} \\ &- \sum_{k=1}^{m}\frac{i\Gamma_{kp}}{2\pi}\frac{1}{c-c^2/\bar{\zeta}_{kp}} - \frac{i\Gamma_{0q}}{2\pi}\frac{1}{c-\zeta_{0q}} + \frac{i\Gamma_{0q}}{2\pi}\frac{1}{c-c^2/\bar{\zeta}_{0q}} - \sum_{k=1}^{m}\frac{i\Gamma_{kq}}{2\pi}\frac{1}{c-\zeta_{kq}} \\ &+ \sum_{k=1}^{m}\frac{i\Gamma_{kq}}{2\pi}\frac{1}{c-c^2/\bar{\zeta}_{kq}} = 0 \end{aligned} \tag{4}$$

and

$$\begin{aligned} -U(e^{-i\alpha} - e^{i\alpha}) &- \frac{i\Gamma_{0p}}{2\pi}\frac{1}{c+\zeta_{0p}} + \frac{i\Gamma_{0p}}{2\pi}\frac{1}{c+c^2/\bar{\zeta}_{0p}} - \sum_{k=1}^{m}\frac{i\Gamma_{kp}}{2\pi}\frac{1}{c+\zeta_{kp}} \\ &+ \sum_{k=1}^{m}\frac{i\Gamma_{kp}}{2\pi}\frac{1}{c+c^2/\bar{\zeta}_{kp}} + \frac{i\Gamma_{0q}}{2\pi}\frac{1}{c+\zeta_{0q}} - \frac{i\Gamma_{0q}}{2\pi}\frac{1}{c+c^2/\bar{\zeta}_{0q}} + \sum_{k=1}^{m}\frac{i\Gamma_{kq}}{2\pi}\frac{1}{c+\zeta_{kq}} \\ &- \sum_{k=1}^{m}\frac{i\Gamma_{kq}}{2\pi}\frac{1}{c+c^2/\bar{\zeta}_{kq}} = 0. \end{aligned} \tag{5}$$

The two point vortices Γ_{0p} and Γ_{0q} will be identified as either 'nascent vortices' or 'Kutta vortices' for each will always represent the first vortex introduced into the flow at each edge of the plate. Furthermore, their strength and location at the start of each step, i.e. at the time of their introduction into the flow, will be such that the Kutta conditions expressed by (4) and (5) will be satisfied. This and other computational details will be explained later.

Formulation of the resistance equations

The forces exerted on a stationary body by a time-dependent flow represented by the complex potential w can be calculated from the generalized Blasius theorem by writing

$$F_p + iF_n = \frac{i\rho}{2}\overline{\oint (dw/dz)^2 dz} + i\rho\frac{\partial}{\partial t}\oint w\,dz, \tag{6}$$

in which F_n and F_p represent the components of force normal and tangential to the plate.

It is convenient to evaluate (6) in two parts by writing

$$X_1 - iY_1 = \frac{i\rho}{2} \oint (dw/d\zeta)^2 (d\zeta/dz)\, d\zeta \tag{7}$$

and

$$X_2 + iY_2 = i\rho \frac{\partial}{\partial t} \left\{ (wz)_{pc} - \oint z(dw/dz)\, dz \right\}, \tag{8}$$

which results from an integration by parts of the second part of (6); $(wz)_{pc}$ is the difference between the values of wz at the beginning and end of the plate contour. Inserting (1) and (2) in (7) and carrying out the indicated integration, one finally has

$$X_1 - iY_1 = \rho \sum_{k=0}^{m} (\Gamma_{kq} v_{kqy} - \Gamma_{kp} v_{kpy}) + i\rho \sum_{k=0}^{m} (\Gamma_{kq} u_{kqx} - \Gamma_{kp} u_{kpx}), \tag{9}$$

in which u_{kqx} and v_{kqy} represent respectively the x and y components of velocity at the centre of the kth q-vortex in the physical ($z = x + iy$) plane. As will be pointed out later, the first sum in (9) is identically equal to zero, i.e. there is no force acting along the plate (known as the leading-edge suction in airfoil theory) and the Cisotti paradox (Birkhoff 1955) does not arise.† The steady component of the normal force reduces to

$$Y_1 = \rho \sum_{k=0}^{m} (\Gamma_{kp} u_{kpx} - \Gamma_{kq} u_{kqx}). \tag{10}$$

The unsteady part of the force, represented by (8), may be evaluated by first noting that $(wz)_{pc}$ is identically equal to zero since there is no jump in the stream function ϕ along the contour, or since the nascent vortices and their images are not connected to the edges of the plate by vortex sheets of finite or vanishingly small vorticity. The remaining integral may be written as

$$X_2 + iY_2 = -i\rho \frac{\partial}{\partial t} \oint \left(\zeta + \frac{c^2}{\zeta} \right) (dw/d\zeta)\, d\zeta, \tag{11}$$

which yields $X_2 = 0$, since $c^2/\zeta_k + c^2/\bar{\zeta}_k$ is real, and

$$Y_2 = 4\pi\rho c^2 (\sin\alpha) \frac{\partial U}{\partial t} + \rho \frac{\partial}{\partial t} \left\{ \sum_{k=0}^{m} \Gamma_{kq} \left(\frac{c^2}{\zeta_{kq}} + \frac{c^2}{\bar{\zeta}_{kq}} \right) - \sum_{k=0}^{m} \Gamma_{kp} \left(\frac{c^2}{\zeta_{kp}} + \frac{c^2}{\bar{\zeta}_{kp}} \right) \right\}. \tag{12}$$

Noting that

$$c^2/\zeta_{kq} + c^2/\bar{\zeta}_{kq} = 2\xi_{ikq},$$

where ξ_{ikq} and η_{ikq} represent the co-ordinates of the image of the kth q-vortex, equation (12) may be reduced to

$$Y_2 = 4\pi\rho c^2 \frac{\partial U}{\partial t} \sin\alpha + 2\rho \frac{\partial}{\partial t} \Sigma (\Gamma_{kq} \xi_{ikq} - \Gamma_{kp} \xi_{ikp}). \tag{13}$$

The term in parentheses may also be expressed in terms of the velocities $u_{ikq\xi}$ and $u_{ikp\xi}$ by performing the indicated timewise differentiation. However, this procedure is hardly necessary and as far as the numerical calculations are concerned the use of (12) is easier and less time consuming.

† This singular-point paradox is not eliminated in Wu (1962).

The sum of equations (10) and (13) yields the total force acting on an inclined plate:

$$F_n = Y_1 + Y_2, \tag{14}$$

which may be expressed in terms of a normal-force coefficient C_n defined as

$$C_n = 2F_n/\rho b U^2 = F_n/2\rho c U^2, \tag{15}$$

where $b = 4c$.

Velocities in the circle and plate plane

Several of the equations obtained thus far require the evaluation of the velocities of the vortex centres. Moreover, the advancement of the position of each vortex in the z plane at the end of each time interval requires the transformation of the positions of all vortices into the circle plane, the calculation of the velocities at each vortex centre in the circle plane and, finally, the reverse transformation of the velocities from the circle to the plate plane. For the velocities in the circle plane this reduces to subtracting from (1) the complex potential corresponding to the vortex, the kth, say, for which the velocity components are to be determined and evaluating the derivative of the remaining terms at $\zeta = \zeta_k$. To determine the velocities in the physical plane, however, one has to subtract $(i\Gamma_k/2\pi)\log(z - z_k)$ from (1) or, in terms of ζ, the terms (see, for example, Sarpkaya 1967)

$$\frac{i\Gamma_k}{2\pi}\log(\zeta - \zeta_k) + \frac{i\Gamma_k}{2\pi}\log\left(1 - \frac{c^2}{\zeta\zeta_k}\right). \tag{16}$$

It should be noted that the first term in (16) is the complex function corresponding to the kth vortex in the ζ plane. The second term appears merely as a consequence of the transformation used. Carrying out the procedure just described, one finally has the following relationship between the velocities of the vortices in the z and ζ planes:

$$-u_{kpx} + iv_{kpy} = (-u_{kp\xi} + iv_{kp\eta})\frac{\zeta_{kp}^2}{\zeta_{kp}^2 - c^2} - \frac{i\Gamma_{kp}}{2\pi}\frac{\zeta_{kp}c^2}{(\zeta_{kp}^2 - c^2)^2} \tag{17}$$

and

$$-u_{kqx} + iv_{kqy} = (-u_{kq\xi} + iv_{kq\eta})\frac{\zeta_{kq}^2}{\zeta_{kq}^2 - c^2} + \frac{i\Gamma_{kq}}{2\pi}\frac{\zeta_{kq}c^2}{(\zeta_{kq}^2 - c^2)^2}, \tag{18}$$

in which

$$-u_{kp\xi} + iv_{kp\eta} = [dw_{kp}(\zeta)/d\zeta]_{\zeta=\zeta_{kp}}, \tag{19}$$

where $w_{kp}(\zeta)$ is given by

$$w_{kp}(\zeta) = w(\zeta) - (i\Gamma_{kp}/2\pi)\log(\zeta - \zeta_{kp}). \tag{20}$$

Expressions similar to (19) and (20) may easily be written for the q-vortices as well as for each of the two nascent vortices with proper attention to their sign or the sense of rotation.

The velocity components given by (17) and (18) together with the Kutta conditions given by (4) and (5) render the X_1 component of the force [the real part of (9)] identically equal to zero. Demonstrating this is rather lengthy and will not be done here. However, if one considers the fact that the Cisotti paradox (Birkhoff 1955) in a Joukowsky flow past a plate is a consequence of the infinite

velocities occurring at the leading edge of the plate, and the fact that in the present analysis the velocities at both the leading and trailing edges of the plate are rendered finite by satisfying the Kutta condition at both points, it is easy to see that there can be no force or leading-edge suction acting on the single points at either end of the plate, i.e. $X_1 = 0$.

3. Method of calculation

Vorticity flux

The rate at which vorticity is shed into the wake is given by

$$\int_0^{\delta} \left(\frac{\partial v}{\partial x} - \frac{\partial u}{\partial y}\right) u\, dy, \tag{21}$$

where δ is the boundary-layer thickness. This may be closely approximated by

$$\partial\Gamma/\partial t = \tfrac{1}{2}(V_1^2 - V_2^2) \simeq \tfrac{1}{2}V_1^2, \tag{22}$$

where V_1 and V_2 represent the velocities at the outer and inner edges of the shear layer. The fact that this simple expression gives a close estimate of the total vorticity flux through each sheet per unit time even for flows with rapidly curving streamlines has been demonstrated by Fage & Johansen (1927, 1928) through numerous experiments with inclined plates, cylinders, wedges and ogival models.

In a discrete-vortex model, (22) may be employed in various ways provided that certain basic and experimentally observed facts are not contradicted, that the numerical procedure used to implement the method is stable, and that the results do not critically depend on the magnitude of the new and hopefully minimum number of disposable parameters introduced. The methods used in the past may be roughly classified into three categories.

The first involves the use of the maximum velocity occurring in the boundary layer near the point of separation (Sarpkaya 1968). This procedure allows a reciprocal action between the wake and the vorticity flux and in turn between the wake and the boundary layer.

The second involves the selection of a suitable fixed point in the flow near the separation point and the use of the velocity U_s at that point to calculate the rate at which vorticity is shed into the wake from (Clements 1973; Clements & Maull 1975; Kuwahara 1973)

$$d\Gamma/dt = \tfrac{1}{2}U_s^2. \tag{23}$$

In this method no interaction is allowed between the shed vortices and the amplitude of oscillation of the point of appearance of the vortices. As discovered by Kronauer (1964) and substantiated by Gerrard (1967), the oscillation of the point of appearance of the vortices is vital to the continuance of oscillations in resistance and is coupled with the manner in which the vortex sheets roll up. This fact was also overlooked by Kuwahara (1973), who fixed the position of the appearance of the nascent vortices. This resulted in violent normal-force oscillations (of varying magnitudes for the angles of incidence considered) wholly unrelated to the shedding of vortices. Evidently, the effect of the departure on

the point chosen from the separation point on the resulting flow characteristics and forces will have to be assessed through separate calculations.

The third category involves the isolation of the shear layer from the separation point (Gerrard 1967), the selection of a control surface downstream of separation and the calculation of the vorticity flux across the control surface through the use of suitable assumptions. In this method, the effects of the vortex sheet upstream of the control surface are ignored and the effect of the disposable parameters on the resulting flow is evaluated through separate calculations.

Apparently, there is not a unique procedure for calculating the rate at which vorticity is shed into the wake and the one which most clearly reproduces the experimentally observed features of the free shear layers must be adopted. Fage & Johansen (1927, 1928), through quite ingenious experiments with various bluff bodies, have shown that vorticity is shed from the two sides of an asymmetric body at the same rate; that the motion in a sheet is steady near the body, except possibly near the inner edge of the shear layers; that fluid flows into a sheet through both edges, but at a greater rate through the outer edge; that at each section of the sheet the velocity rises from a small value to a well-marked maximum value (approximately $V_1/U = 1{\cdot}45$) and then very slowly decreases to about 1·35 within a distance of approximately $y \simeq 2c$, where the breadth of the sheet reaches a value $\Delta \simeq c$; and, finally, that the velocity V_1 at the outer edge of the sheet is much larger than the velocity V_2 at the inner edge and V_2^2 may be ignored in (22) in calculating the vorticity flux.

In the present model, as it is applied to a flow about an inclined plate, the vorticity could have been calculated, at each time interval, through the use of the mathematically finite velocity occurring at the edge of the plate. This is a plausible but not a numerically stable procedure since the separation points are singularities of the transformation used. This difficulty has also been noted by Clements (1973).

It is apparent from the foregoing discussion of the various procedures used in the determination of the vorticity flux and the experimentally observed characteristics of the free shear layers that a new method will have to be devised which will make the use of the Kutta conditions possible and will permit a reciprocal action between the wake and the vorticity flux. The simplest and most direct procedure which will make these considerations possible is the use of the velocity U_{sh} in the shear layers by writing

$$\partial\Gamma/\partial t = \tfrac{1}{2}U_{sh}^2. \tag{24}$$

Then the question arises as to what is meant by U_{sh} in a shear layer approximated by discrete vortices which have different constant strengths. The use of the velocity at the position of a single vortex (with $k = 1$, say) would not be satisfactory partly because Γ_{1p} or Γ_{1q} vortices are too close to the edges of the plate and the radii of curvature of their pathlines are relatively small. Thus the numerical errors involved in the determination of their transport velocities could give rise to unacceptable oscillations in the vorticity flux. One would, therefore, abandon this idea in favour of using the average of the transport velocities of a number of vortices in each shear layer. This will not only smooth

out any numerical errors but will also give a better representation of the velocity and vorticity flux in the shear layers. Thus the decision to be made concerns the number of vortices whose average transport velocity is to be taken as U_{sh}. It is clear at the outset that k or $k\Delta t$ cannot be too large. First, if k were too large the kth vortex would be either in or very close to the first vortex cluster. Second, if $k\Delta t$ were too large, larger than the period of vortex shedding, then the interaction between the wake and the free shear layers would be lost. Several preliminary calculations have shown that taking U_{sh} as the average of the velocities of the first four vortices ($k = 1$–4) will be quite satisfactory and that the results would not materially differ if one used three or six vortices. The decision to use only the first four vortices was based partly on the fact that the fourth vortex is located at about $y \simeq c$ and that the breadth of the actual shear layers at $y \simeq c$ is rather small and, more important, there is a well-defined shear layer. Furthermore, the time interval during which four vortices are introduced into the flow is about $\frac{1}{15}$ of the period of vortex shedding. This time interval is sufficiently small that during it U_{sh}, as calculated above, can respond to the changes in the wake. Finally, the number of vortices used must be small enough to allow the nascent vortices to respond to the changes in the shear layers without too large a phase lag. In conclusion then, the strength of each new vortex at each shear layer was calculated through the use of (24). In the p-layer, $U_{sh} = U_{shp}$, the average of the velocities of four p-vortices in this layer, i.e.

$$U_{shp} = \frac{1}{4} \sum_{k=1}^{4} (u_{kp}^2 + v_{kp}^2)^{\frac{1}{2}}. \tag{25}$$

For the other shear layer, U_{shq} is calculated in the same manner.

Suffice it to say on this very important aspect of the discrete-vortex model that the procedure described above recognizes the possibility of an oscillation in the rate of shedding of circulation even without an oscillating wake, permits a reciprocal action between the shear layers and the wake, and finally reduces the number of disposable parameters in the calculation of the vorticity flux to one, the number of vortices near the origin of the shear layers.

Introduction, convection, cancellation and combination of vortices

The introduction, as well as the subsequent convection, of the nascent vortices is of major importance in the evolution of the entire wake. They must be introduced at sufficiently small time intervals and convected in such a manner that they can reasonably follow the true streamlines in regions of flow where the radius of curvature of the streamlines is small. Their strength and position must be such that the Kutta conditions are satisfied at the start of each time interval and that their point of appearance reacts to and interacts with the motion of the wake.

To explain the method let us consider a particular time t after the start of the motion and assume t to be sufficiently large that there are at least four vortices in each shear layer. Then the appearance and convection of vortices proceeds as follows.

(*a*) Calculate U_{shp} and U_{shq} from (25).

(*b*) Calculate $\Delta\Gamma_{0p}$ and $\Delta\Gamma_{0q}$ from $\Delta\Gamma_{0p} = \frac{1}{2}U_{shp}^2\Delta t$ and $\Delta\Gamma_{0q} = \frac{1}{2}U_{shq}^2\Delta t$.

(*c*) Calculate the positions ζ_{0p} and ζ_{0q} of the nascent vortices Γ_{0p} and Γ_{0q} from (4) and (5). A careful examination of these equations shows that ζ_{0p} and ζ_{0q} may be calculated through the use of a suitable iteration scheme.

(*d*) Calculate the velocities at the position of each vortex ($k = 0$–m) through the use of (17) and (18).

(*e*) Convect only the vortices Γ_{1p} and Γ_{1q} for a time interval $\frac{1}{5}\Delta t$ using the expressions

$$\left.\begin{aligned} x(t+\tfrac{1}{5}\Delta t) &= x(t)+\tfrac{1}{5}u(t)\,\Delta t,\\ y(t+\tfrac{1}{5}\Delta t) &= y(t)+\tfrac{1}{5}v(t)\,\Delta t. \end{aligned}\right\} \tag{26}$$

(*f*) Repeat steps (*d*) and (*e*) five times.

(*g*) Calculate the velocities at the centres of all the vortices and convect the vortices with $k = 2$–m for a time interval Δt using expressions similar to (26).

(*h*) Repeat steps (*a*)–(*g*) five times.

(*i*) At the end of the fifth interval, i.e. at $\Delta T = 5\Delta t$, call $\Gamma_{0p} = \Gamma_{1p}$ and $\Gamma_{0q} = \Gamma_{1q}$. In other words, at every $5\Delta t$ a new vortex of permanent character is born. Obviously, at the end of any time interval Δt there is only one nascent vortex and the Kutta condition is satisfied in some mean sense only since the flow is unsteady.

The most important features of the foregoing procedure are that considerable attention is paid to the motion of the first vortex, where the streamlines are rapidly curving, and that both the rate at which vorticity is shed into the wake and the position at which this vorticity appears are allowed to vary with time.

The description of the introduction and convection of the vortices would not be complete without an explanation of the introduction of the first four vortices, which enable the model to calculate the rate at which vorticity is shed into the wake and sustain the evolution of the wake. The fluid was set in motion impulsively from rest. Thus, initially, there was no vorticity in the fluid and a simple method had to be devised to generate the first four vortices in each shear layer. For this purpose, it was decided to rely on the experimental facts established by Fage & Johansen (1927, 1928) rather than on some other plausible but nevertheless arbitrary procedure. As stated earlier, the velocity V_1 in a shear layer in a steady flow is about $1{\cdot}4U$ and the vorticity flux may be calculated from $\Delta\Gamma \simeq \frac{1}{2}V_1^2\Delta t$. Thus $\Delta\Gamma \simeq \Delta t$. Accordingly, the strengths Γ_{1p} and Γ_{1q} of the first vortices were taken equal to $5\Delta t$ and these vortices placed on the x axis in accordance with (4) and (5). Then they were convected in five steps at time intervals of $\frac{1}{5}\Delta t$. Then two nascent vortices of strengths $\Delta\Gamma_{0p} = \Delta\Gamma_{0q} = \Delta t$ were introduced at time intervals of Δt as previously described and the first vortices were further convected for a time interval Δt. At time $5\Delta t$, the last nascent vortices became the first vortices and the previously introduced and convected vortices became the second vortices. The foregoing procedure was repeated four times, i.e. until there were four vortices in each shear layer. Then the calculations proceeded as described in steps (*a*)–(*i*).

The above method of starting the calculations may be discussed at length in

terms of the initial values of $\partial\Gamma/\partial t$, the radius of curvature of the initial streamlines, etc. In fact, at one time during the evolution of the method an attempt was made to use the spiral form of the shear layers at small times as determined by Wedemeyer (1961). The analysis had first to be applied to an inclined plate since Wedemeyer's analysis was carried out only for $\alpha = \frac{1}{2}\pi$. Then four vortices of equal strength were placed on the spiral in such a manner that the Kutta conditions were satisfied. It was soon discovered that this laborious procedure did not produce results noticeably different from those of the one finally adopted herein. In fact, there were no differences in the vortex strengths and positions after the tenth vortex.

Three additional features of the model concern the removal and coalescence of vortices and the massing of the effects of clusters of point vortices into those of an equivalent single vortex. The vortices which approach too close to the rear of the plate will ordinarily be dissipated by the action of viscosity as first noted by Fage & Johansen (1927). In the absence of viscosity and the no-slip condition, such vortices can acquire extremely large velocities. Thus, they had to be removed from the calculation whenever they came nearer than $0{\cdot}1c$ to the rear face of the plate. In passing it should be observed that a line vortex which has been in the wake of a viscous flow with a Reynolds number of about 40000 for a period $t = 8c/U$ will have a core radius of approximately $0{\cdot}07c$ according to Schaefer & Eskinazi (1959). Thus the distance $0{\cdot}1c$ is of the order of the core radius of a decaying vortex.

As for the coalescence of vortices, it has been recognized (Gerrard 1967; Moore 1971, 1974; Chorin & Bernard 1972; among others) that the orbiting motion of point vortices can rapidly affect neighbouring vortices and that vortices of opposite circulation could remove themselves from the wake at high speeds when in close proximity. This was avoided by coalescing such vortices for $k > 20$ with a separation of less than $0{\cdot}1c$, i.e. by combining the two vortices into an equivalent single vortex.

In real flows only a fraction (say about 60 %) of the circulation fed into the shear layers is found in the vortex clusters or in the concentrated vortices of the Kármán vortex street (see, for example, Mair & Maull 1971). In the absence of such a viscous and/or turbulent dissipation, the loss of vorticity at the rear face of the plate and "a small amount of cancellation between elementary vortices of opposite sign which enter the same rolled-up vortex core" (Clements 1973) are the only two mechanisms which could bring about some loss in circulation in the concentrated vortices. Evidently, these two mechanisms are not sufficient to account for an approximately 40 % loss in circulation. This led Clements (1973) to reason that the mechanism whereby much of the vorticity is lost must be viscous in nature.

Finally, the limitations imposed on the calculations by the size of the computer used (IBM-360/67) and the computer time available (maximum 2 h per run) made it necessary to combine the point vortices in a given cluster into an equivalent single vortex whose strength was the sum of the individual strengths and whose position was the centre of vorticity of the cluster. This procedure was used when a cluster passed downstream beyond about $y/c = 8$. Exploratory

calculations with or without such a combination have shown that C_n is not noticeably affected and that the method of combination should be used to save computer time and to produce a simple and clean picture of the vortex street.

Time interval

The selection of an optimum time interval was of primary importance in achieving a relatively time-step insensitive result and in saving computation time. A large number of calculations have been repeated with a single program by changing only the time step. The time steps are given in terms of a normalized time t which is related to the real time t_r by $t = Ut_r/c$. Experiments on Δt began with $\Delta t = 0{\cdot}16$ and were repeated with $\Delta t = 0{\cdot}08$, $0{\cdot}04$ and $0{\cdot}02$. The results showed that $\Delta t = 0{\cdot}16$ was too large and that the results with $\Delta t = 0{\cdot}08$, $0{\cdot}04$ and $0{\cdot}02$ did not significantly differ. However, the computation time required with $\Delta t = 0{\cdot}02$ was about ten times larger than that with $\Delta t = 0{\cdot}04$. In view of the fact that a new vortex is introduced into the wake every $5\Delta t$, all the calculations reported herein were made with $\Delta t = 0{\cdot}04$.

The normalized circulation Γ/Uc of the point vortices in the wake took values from about $0{\cdot}16$ to $0{\cdot}40$. This was about 1–3 % of the total circulation found in a vortex cluster.

In closing the description of the method, a few additional comments must be made. First, in advancing the position of the vortices, two additional schemes were tried through the use of either

$$x(t+\Delta t) = x(t-\Delta t) + 2\Delta t\, u(t)$$

or† $$x(t+\Delta t) = x(t) + \tfrac{1}{2}[3u(t) - u(t-\Delta t)]\,\Delta t.$$

These did not lead to any noticeable differences since to begin with Δt was chosen sufficiently small. Second, the normal force acting on the plate was calculated from the positions, velocities and strengths of the vortices at every Δt using (10), (13) and (14). Third, no initial perturbations had to be introduced into the flow since the flow was inherently asymmetric and capable of generating an alternating vortex street. Finally, the first sum in (8) was calculated and printed at every Δt. The calculations showed that the maximum values of $X_1/\rho U^2 c$ were less than 10^{-4}.

4. Results and comparison with experiments

Computations were made for angles of attack from 40 to 80° at 10° intervals. The detailed discussion of the results and their comparison with the experiments will be confined to $\alpha = 50°$, in the interest of space, and additional comments will be presented for other angles of attack.

The computer programs provided, at any time specified, the positions of all the vortices, the rate of shedding of vorticity into the shear layers from the leading and trailing edges of the plate, and the normal-force coefficient given

† Similar expressions are used for $y(t)$.

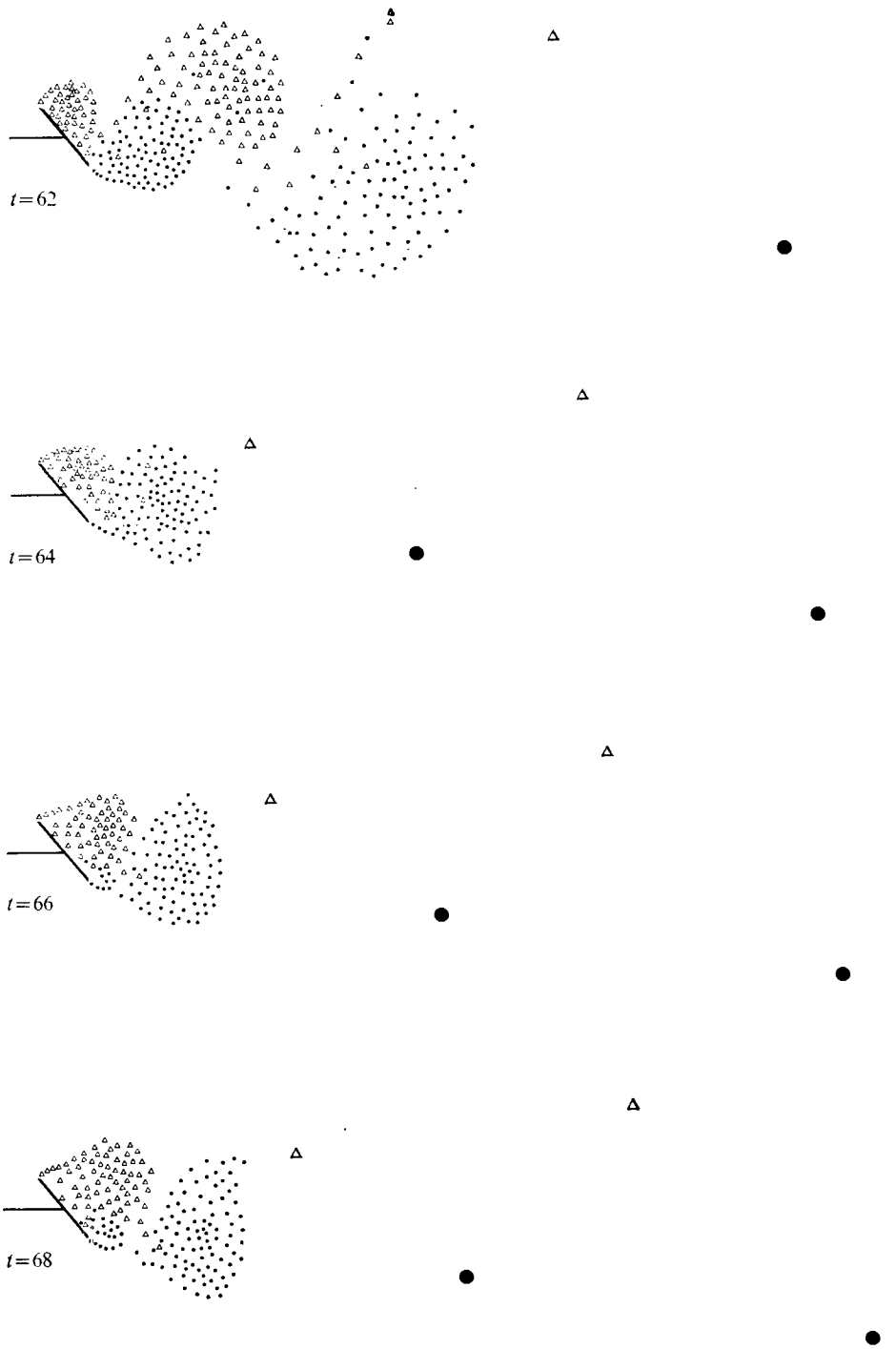

FIGURE 2. For legend see next page.

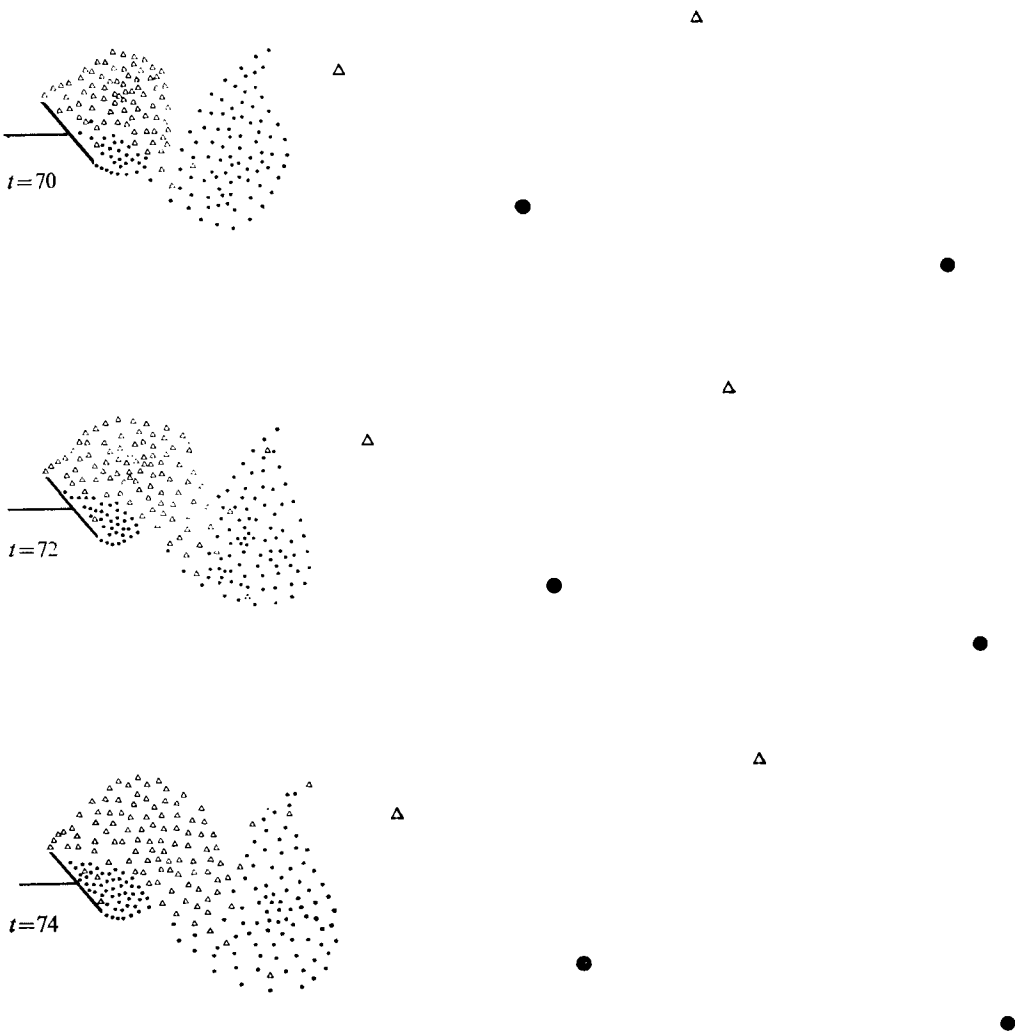

FIGURE 2. Vortex arrangements over one half-cycle of steadily periodic flow ($\alpha = 50°$). ●, positive vortices; △, negative vortices.

by (15). The vortex shedding frequency was calculated using the period of oscillations in $d\Gamma/dt$ when the flow has attained a steady or nearly steady state.

Figure 2 shows the evolution of the wake during a particular time interval and the replacement of vortex clusters or shed system of vortices by equivalent single vortices. Figures 3, 4 and 5 (plates 1 and 2) show the vortex shedding at times $t = 48$, 62 and 74, respectively. Figures 4 and 5 correspond to the first and last frames in figure 2. The pictures were taken with a thin flat plate 3·75 cm wide (see Sadler (1973) for a detailed description of the experimental apparatus) immersed in a channel 90 cm wide and 15 cm deep. The flow was started nearly impulsively from rest and visualized with aluminium powder. The Reynolds number of the asymptotic steady flow was about 11 000. The evolution of the

wake from the start of the motion was photographed with a high-speed cine camera. Figures 3, 4 and 5 correspond to three frames of such a particular motion picture at times $t = 48$, 62 and 74 respectively.

A comparison of figures 4 and 5 with the corresponding frames in figure 2 show that the agreement between the positions of the vortex clusters and shear layers predicted numerically and those observed experimentally for $\alpha = 50°$ is quite good. Equally satisfactory agreement was obtained for all the other angles of attack studied herein. In fact, it may be said that the simulation of the actual wake flow of a real fluid by a simplified model within the framework of potential flow theory accounts for the essential features of a very complicated process not only in the far wake, where the effect of discretization of the shear layers should be rather small, but also in the near wake, where the rolling up of the shear layers is strongly dependent on the instantaneous distribution of vorticity and the process of viscous dissipation. However, the validity of the model cannot be fully justified by the agreement with the experimental observations of the kinematics of the flow field alone. There must be an equally satisfactory agreement between the observed and predicted dynamic characteristics (i.e. Strouhal numbers, drag coefficients, vortex strengths, etc.) of the flow.

The rate of shedding of vorticity into the shear layers emanating from the leading and trailing edges of a plate set at an angle of attack of 50° is shown in figure 6. At $t = 0$, $\partial\Gamma/\partial t = 1$ because of the way the first four vortices are introduced into the shear layers. Apparently, following the initial period of flow establishment, equal amounts of vorticity are shed during each cycle from each edge of the plate. This is in conformity with the measurements of Fage & Johansen (1927, 1928). It is also apparent that this rate varies periodically with an amplitude of about $\frac{1}{4}\overline{\partial\Gamma/\partial t}$ about a mean value of unity (U and c are taken equal to unity). Fage & Johansen (1927) found no oscillations in V_1 (the velocity at the outer edge of the shear layer) but recorded non-periodic oscillations in velocity at points well within the shear layer. The measurements of Fage & Johansen (1928) have also shown that the mean vorticity flux increases from 0·92 for $\alpha = 30°$ to 1·10 for $\alpha = 90°$, with an expected intermediate value of 0·99 for $\alpha = 50°$. The present calculations yielded a mean value of $\overline{\partial\Gamma/\partial t} \simeq 0{\cdot}96$ for $\alpha = 40°$ and nearly unity for all other angles of attack. In terms of the average shear-layer velocity U_{sh}, the above angles correspond to $U_{sh} = 1{\cdot}41$ for $\alpha > 50°$ and to $U_{sh} = 1{\cdot}39$ for $\alpha = 40°$. The periodic oscillations in the vorticity flux correspond to changes in U_{sh} from approximately 1·2 to 1·6. During a given cycle, the lowest value of U_{sh} in a given shear layer occurs when a vortex cluster is about to break away from that shear layer [see figure 7 (plate 2) and frames 2 and 7 in figure 2]. The maximum value of U_{sh} also occurs at the same time but in the other shear layer. In other words, one vortex cluster at a given edge is fed the largest amount of vorticity when another cluster in the vicinity of the opposite edge is just about to break away from the layer which feeds it.

Similar oscillations in the vorticity flux have been observed by others (e.g. Sarpkaya & Garrison 1963; Gerrard 1967; Chaplin 1973; Clements 1973) in connexion with flow about bluff bodies of different shapes. For example, Clements (1973) found periodic oscillations with an amplitude of about 0·20 $\overline{\partial\Gamma/\partial t}$ about a

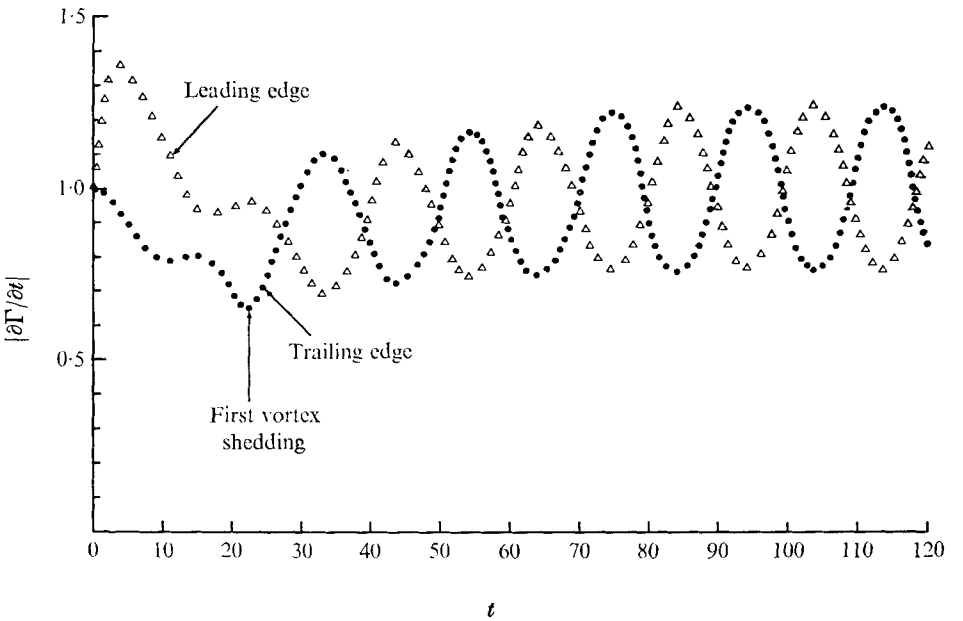

FIGURE 6. Rate of shedding of vorticity into shear layers from the leading and trailing edges of the plate ($\alpha = 50°$). Note that the weakest and the strongest vortices are shed from the plate at the start of the motion from the trailing and leading edges respectively.

mean value of 0·765 for a flow in the near wake of a square-based bluff body. It should be noted in passing that the mean vorticity flux obtained by Clements (1973) is quite comparable with that measured by Fage & Johansen (1927) for a similar based body (i.e. an extended ogival shape).

The Strouhal number of the vortex shedding was determined from figures similar to figure 6 by taking the inverse of the average period of the last two or three full cycles of oscillation. In the range of $40° < \alpha < 80°$, which was also the range of calculations, it was found that

$$S = 4fc \sin\alpha/U = 0{\cdot}154 \pm 0{\cdot}003.$$

Over the same range, Fage & Johansen found $S = 0{\cdot}148 \pm 0{\cdot}003$ with a tunnel-height to plate-chord constriction ratio of $K = 14$. Abernathy (1962) obtained $S = 0{\cdot}164$ for $K = 13{\cdot}98$. The Strouhal numbers obtained herein may be considered in good agreement with those obtained experimentally in view of the fact that the Strouhal number for a given body decreases to a minimum with increasing constriction ratio and that the experimental values for the same constriction ratio may vary with the end conditions of the model (Fage & Johansen 1927, 1928; Abernathy 1962), with the intensity and scale of turbulence of the ambient flow (Schubauer & Dryden 1935), and possibly with the diffusion and strength of the shed cluster of vortices. The last possibility, which is also closely related to the mechanism of vorticity loss in real and computed flows, needs to be further discussed.

The calculations have shown that the strength of the vortex clusters varies from 84 to 91 % of the vorticity generated in each shear layer, the 10–15 %

loss in vorticity arising from the removal of vorticity at the rear face of the plate and a small amount of cancellation between elementary vortices of opposite sign which enter the same rolled-up vortex core. The corresponding experimental values for flat plates, cylinders and many other types of bluff bodies vary from about 50 to 66 % (Fage & Johansen 1927, 1928; Mair & Maull 1971). Thus, the vortex clusters of the present model are about 50 % stronger than those found in real flows under similar circumstances. Clements (1973) has arrived at essentially the same conclusions. The large discrepancy between the experiments and calculations is undoubtedly due to the difference in the mechanisms whereby vorticity is lost. In real flows, part of the vorticity is lost immediately behind the plate by viscous action and by mixture of the positive and negative vorticity from the two edges of the plate, and part in the shedding process, during which the vortex cluster to be shed attains its minimum transport velocity and draws oppositely signed vorticity across from the other side of the wake (Gerrard 1967). In fact, it is conjectured that the loss in vorticity depends on the particular time in a given cycle and reaches its maximum rate just at the time of shedding as defined previously. The numerical model cannot simulate such a kinematic- or eddy-viscosity dependent phenomenon. If necessary, an additional loss in vorticity will have to be artificially introduced into the model, beyond and above that produced by the two mechanisms cited above, in order to bring the strengths of the shed vortex clusters into closer agreement with those obtained experimentally. It appears that the Strouhal number does not strongly depend on the strength of the shed cluster of vortices.

Among several other parameters such as the velocity distributions in time or space, the positions of the vortices, etc., which could have been compared with those obtained experimentally, the normal force acting on the plate was thought to be the most significant one both from a practical and analytical viewpoint. The coefficient C_n was calculated, as described previously, at suitable time intervals and plotted as a function of the normalized time t. Figure 8 shows the normal-force coefficient for $\alpha = 50°$. Force coefficients for other angles of attack are quite similar in character and vary only in their asymptotic values.

Following a period of rapid rise, the normal-force coefficients exhibit significant oscillations in response to the vortex shedding. These oscillations, which have a frequency nearly equal to twice the vortex shedding frequency, decrease to about 10 % of the average value of C_n in magnitude as the number of vortices in the wake increases. Finally, for $\alpha = 50°$, C_n approaches an asymptotic value of about 2. Table 1 gives the asymptotic values of C_n obtained in the present analysis and those obtained experimentally by Fage & Johansen (1927).†

The classical theory of Kirchhoff and Rayleigh (see Lamb 1945, pp. 99–103) predicts a normal-force coefficient $C_n = 2\pi \sin\alpha/(4 + \pi \sin\alpha)$, which is about half that measured by Fage & Johansen (1927). Furthermore, the model is known to be unrealistic in specific details.

Flachsbart (1932) measured a value of $C_n = 1{\cdot}96$ for $\alpha = 90°$ which was independent of the flow Reynolds number $4Uc/\nu$ in the range 6×10^3–6×10^5.

† The C_n values obtained by Fage & Johansen (1927) have been corrected for the wind-tunnel interference as suggested by Glauert (see Fage & Johansen 1927, p. 196).

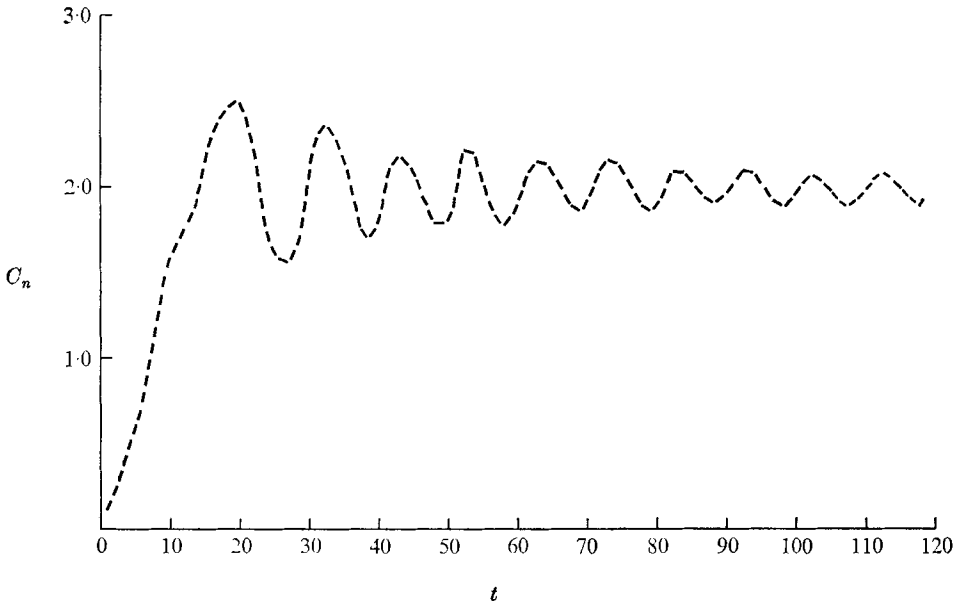

FIGURE 8. The variation of the normal-force coefficient with time in transient and asymptotically steady separated flow over an inclined plate ($\alpha = 50°$).

α (deg)	C_n (present study)	C_n (Fage & Johansen 1927)
40	1·75	1·45
50	2·00	1·65
60	2·25	1·80
70	2·35	1·84
80	2·40	1·86

TABLE 1

Although fairly independent of Reynolds number, the normal-force coefficient is known to depend on the tunnel–plate constriction coefficient and on the turbulence intensity of the ambient flow. Schubauer & Dryden (1935) have shown that turbulence does lower the pressure in the wake and increases the drag coefficient, by perhaps affecting the stability of the shear layers.

The calculated asymptotic values of C_n are 20–25 % larger than those measured by Fage & Johansen (1927). The only explanation which may be offered for this large discrepancy is that the strength of the shed vortex clusters is about 50 % larger than that found in real flows. This view is strengthened by the fact that the model predicts fairly well the kinematics of the flow and the Strouhal number. Attempts made to incorporate into the model an artificial viscous and/or turbulent diffusion of vorticity (ageing the vortices, systematically reducing the strength of the shed vortex clusters, etc.) will not be described here. An appropriate reduction in the strength of the vortices, particularly in the near wake,

did bring about a reduction in the normal force. The important fact is that the discrete-vortex approximation predicts the normal-force coefficient with a 20 % error only even without an artificial reduction in the strength of the shed vortices.

5. Conclusions

A discrete-vortex approximation has been used to model the surfaces of discontinuity, or coherent vortex sheets, and the vortex cores in a two-dimensional flow past an inclined flat plate. The essential characteristics of the model are contained in the use of the Kutta condition and in the determination of the rate of shedding of vorticity from the average of the instantaneous transport velocities of the first four vortices. Both the rate at which vorticity is shed into the wake and the position at which this vorticity appears are allowed to vary with time. The model predicts fairly satisfactorily the Strouhal number and the kinematic features of the flow. The calculated normal-force coefficients are about 20 % larger than those obtained experimentally. In spite of this, however, the discrete-vortex model emerges as one of the most powerful tools in establishing a link between the characteristics of the wake, the body shape and the resulting forces with relatively few disposable parameters such as the time step and the number of vortices used in calculating the mean velocity in each shear layer. No other analytical or numerical model has yet been able to produce equally satisfactory results at sufficiently large Reynolds numbers.

This work formed a part of a broad programme of research in unsteady flow past bluff bodies and financially supported by the National Science Foundation. The author is grateful to the referees for valuable suggestions and comments and to Dr R. R. Clements and Dr D. J. Maull for an advance copy of their paper 'The representation of sheets of vorticity by discrete vortices'.

REFERENCES

ABERNATHY, F. H. 1962 Flow over an inclined plate. *J. Basic Engng, Trans. A.S.M.E.* D **84**, 380.

BIRKHOFF, G. 1955 *Hydrodynamics, A Study in Logic, Fact, and Similitude*, p. 18. Dover.

CHAPLIN, J. R. 1973 Computer model of vortex shedding from a cylinder. *Proc. A.S.C.E. Hyd. Div.* **99**, 155.

CHORIN, A. J. & BERNARD, P. S. 1972 Discretization of a vortex sheet with an example of roll-up. *College of Engng, University of California, Berkeley, Rep.* FM-72-5.

CLEMENTS, R. R. 1973 An inviscid model of two-dimensional vortex shedding. *J. Fluid Mech.* **57**, 321.

CLEMENTS, R. R. & MAULL, D. J. 1975 The representation of sheets of vorticity by discrete vortices. *Prog. Aero. Sci.* **16** (to appear).

FAGE, A. & JOHANSEN, F. C. 1927 On the flow of air behind an inclined flat plate of infinite span. *Proc. Roy. Soc.* A **116**, 170.

FAGE, A. & JOHANSEN, F. C. 1928 The structure of the vortex sheet. *Phil. Mag.* **7** (7), 417.

FLACHSBART, O. 1932 Messungen an ebenen und gewölbten Platten. *Ergebn. Aerodyn. Versuchsanstalt Göttingen*, **4**, 96.

GERRARD, J. H. 1967 Numerical computation of the magnitude and frequency of the lift on a circular cylinder. *Phil. Trans.* A **261**, 137.

KRONAUER, R. E. 1964 *I.U.T.A.M. Conf. on Concentrated Vortex Motions.*

KUWAHARA, K. 1973 Numerical study of flow past an inclined flat plate by an inviscid model. *J. Phys. Soc. Japan*, **35**, 1545.

LAMB, H. 1945 *Hydrodynamics*, 6th edn. Dover.

MAIR, W. A. & MAULL, D. J. 1971 Bluff bodies and vortex shedding – a report on Euromech 17. *J. Fluid Mech.* **45**, 209.

MOORE, D. W. 1971 The discrete vortex approximation of a finite vortex sheet. *Calif. Inst. Tech. Sci. Rep.* AFOSR-TR-72-0034.

MOORE, D. W. 1974 A numerical study of the roll-up of a finite vortex sheet. *J. Fluid Mech.* **63**, 225.

ROSENHEAD, L. 1931 The formation of vortices from a surface of discontinuity. *Proc. Roy. Soc.* A **134**, 170.

SADLER, L. H. 1973 Flow about an oscillating cylinder and frequency synchronization. M.S. thesis, Naval Postgraduate School, Monterey.

SAKS, A. H., LUNDBERG, R. E. & HANSEN, C. W. 1967 A theoretical investigation of the aerodynamics of slender wing–body combinations exhibiting leading-edge separation. *N.A.S.A. Current Rep.* no. 719.

SARPKAYA, T. 1967 Separated unsteady flow about a rotating plate. In *Developments in Mechanics* (ed. J. E. Cermak & J. R. Goodman), vol. 4, p. 1485. Colorado State University.

SARPKAYA, T. 1968 An analytical study of separated flow about circular cylinders. *J. Basic Engng, Trans. A.S.M.E.* D **90**, 511.

SARPKAYA, T. & GARRISON, C. J. 1963 Vortex formation and resistance in unsteady flow. *J. Appl. Mech., Trans. A.S.M.E.* **30**, 16.

SCHAEFER, J. W. & ESKINAZI, S. 1959 An analysis of the vortex street generated in a viscous fluid. *J. Fluid Mech.* **6**, 241.

SCHUBAUER, G. B. & DRYDEN, H. L. 1935 The effect of turbulence on the drag of flat plates. *Nat. Bur. Stand. Rep.* no. 546, p. 129.

WEDEMEYER, E. 1961 Ausbildung eines Wirbelpaares an den Kanten einer Platte. *Ing. Arch.* **30**, 187.

WU, T. Y. 1962 A wake model for free-streamline flow theory. Part 1. Fully and partially developed wake flows and cavity flows past an oblique flat plate. *J. Fluid Mech.* **13**, 161.

FIGURE 3. Photograph of the vortex pattern at $t = 48$ in the wake of a plate set at an angle of attack of 50°.

FIGURE 4. Photograph of the vortex pattern at $t = 62$ in the wake of a plate set at an angle of attack of 50°. This should be compared with the first frame in figure 2.

FIGURE 5. Photograph of the vortex pattern at $t = 74$ in the wake of a plate set at an angle of attack of 50°. This should be compared with the last frame in figure 2.

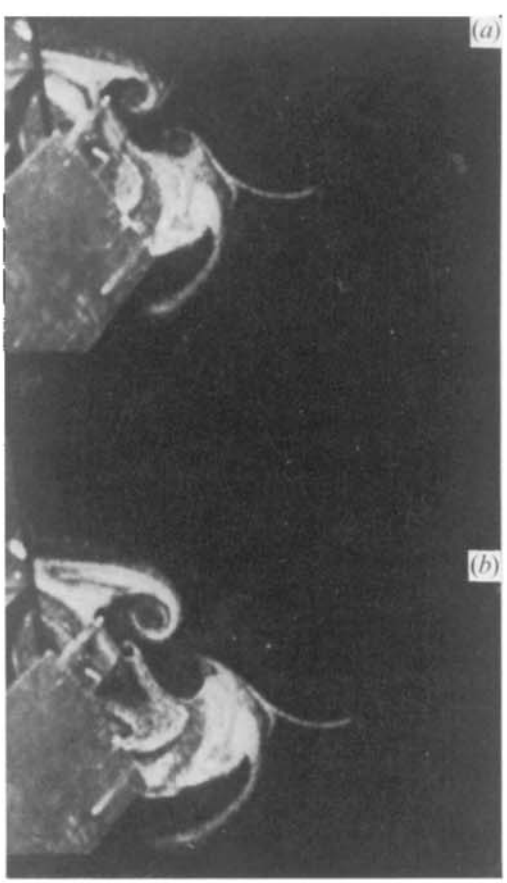

FIGURE 7. Photograph showing the breaking away from its shear layer of the first trailing-edge vortex cluster ($\alpha = 50°$). (*a*) $t = 15$. (*b*) $t = 22$.